Influence of filament spirality on current–voltage characteristics of twisted multifilamentary NbTi superconductors

M. Polák, R.G. Mints* and M. Majoroš

Electrotechnical Institute, Electro-Physical Research Center, Slovak Academy of Sciences, 842 39 Bratislava, Dubravska 9, Czechoslovakia

Received 26 October 1988; revised 16 March 1989

It is shown experimentally, that the current–voltage characteristics of a twisted NbTi multifilamentary superconductor placed in a perpendicular magnetic field differ from those of untwisted superconductors. It was explained by the current transfer across the normal metal matrix due to the inhomogeneous electric field distribution along each filament. Electric field inhomogeneities along each filament arise as a result of varying the angle between the external magnetic field and filament axis. Several model conductors were prepared to investigate the role of the normal metal matrix resistivity and the geometrical arrangement of filaments. A two-dimensional theoretical model explaining the measured characteristics is also presented.

Keywords: superconductors; NbTi; current–voltage characteristics; filament spirality

At present correlation between irregularities in filament cross-sectional area, 'necking' or 'sausaging', and the shape of superconductor current–voltage characteristics has been extensively studied[1-5]. The shape of the electric field *versus* current (E–I) characteristic is quantified in terms of the resistive transition parameter, n, defined by $E \sim I^n$. Filament necking depresses the critical current of the filament locally, which forces the current to transfer across the normal matrix material into neighbouring filaments. In this Paper we show that similar current transfer also arises in the case of entirely homogeneous but twisted filaments.

Previously[6] it was shown that when one separated homogeneous spiral superconducting NbTi filament carrying a constant current and placed in a magnetic field, the local critical current and electric field varied as the angle between the magnetic field and filament axis changed.

In the case of multifilamentary composites the inhomogeneous electric field distribution along each filament in the composite caused current transfer between filaments through the normal metal matrix. Therefore the current–voltage characteristics of the twisted composite can differ from those of the individual filament. Current–voltage (E–I) characteristics measured on different model samples made from homogeneous NbTi filaments are presented. The effect of twisting on E–I characteristics is also demonstrated on one type of NbTi multifilamentary superconductor. The results obtained are in qualitative agreement with predictions of the proposed two-dimensional theoretical model.

Samples

To determine the influence of an inhomogeneous electric field distribution along the spiral filament on the E–I characteristics of the composite, simple model samples with one layer of filaments were made. All of them were made from NbTi copper-stabilized monofilament CFTH-14 (Thomson–Brandt, France). The outer diameter of this superconductor was 52 μm and the filament diameter 36 μm. The parameters of the prepared model samples are given in *Table 1*.

Sample 1 consists of ten spirals of CFTH-14 superconductor tightly wound around the insulated stainless steel tube with an outer diameter of 1.1 mm (*Figure 1*). Spirals were soldered together by Pb–Sn solder. Samples

Table 1 Physical parameters of the one-layer model samples

Sample	Filament	Outer diameter (mm)	Twist pitch (mm)	Filament number
1	CFTH-14	1.1	0.5	10
2	,,	0.17	∞	6
3	,,	0.17	2.57	6
4	,,	2.1	8	53
5	,,	2.2	6.4	36

*On leave from the Institute of High Temperatures, USSR Academy of Sciences, 127 412 Moscow, USSR

0011-2275/89/100963-08 $03.00
© 1989 Butterworth & Co (Publishers) Ltd

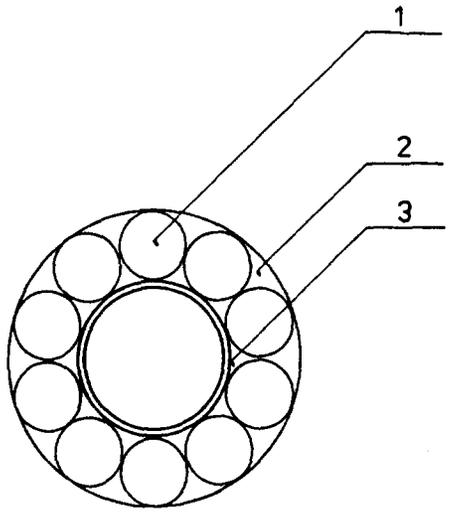

Figure 1 Schematic of sample 1 cross-section: 1, CFTH-14 monofilament; 2, Pb–Sn solder; 3, stainless steel tube

2 and 3 were made from six CFTH-14 filaments located around one central constantan wire (see *Figure 2*). While sample 2 was untwisted, the filaments forming sample 3 were twisted, with a twist pitch, $l_p = 2.57$ mm. In both samples the superconducting filaments and central core were soldered together. A microphotograph of sample 3 is shown in *Figure 3*.

To investigate the influence of the resistance between filaments on the *I–E* characteristics of the model composite conductor twisted samples 4 and 5 were prepared. Sample 4 consists of 53 CFTH-14 wires and 53 copper wires with 45 μm in diameter wound on a stainless steel tube, 2 mm in diameter, and soldered by Pb–Sn (*Figure 4*). Sample 5 consists of 36 CFTH-14 wires and 36 resistive (constantan) wires also wound on a 2 mm stainless steel tube and soldered by Pb–Sn solder. The cross-section of this sample was very similar to that shown in *Figure 4*. Also samples made of a real three dimensional multifilamentary composite containing 37 filaments with diameter 10 μm have been prepared. Twisted, twist pitch 1 mm, as well as untwisted samples have been measured (samples 6 and 7).

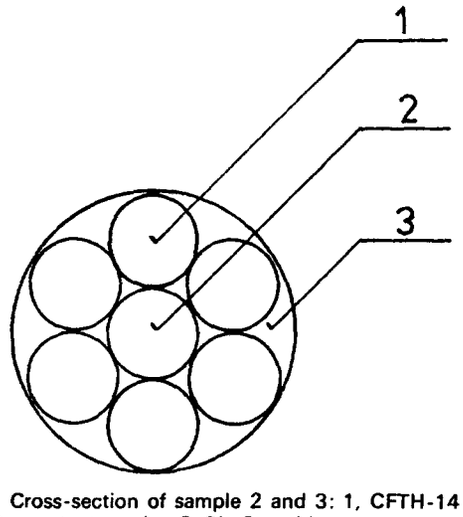

Figure 2 Cross-section of sample 2 and 3: 1, CFTH-14 monofilament; 2, constantan wire; 3, Pb–Sn solder

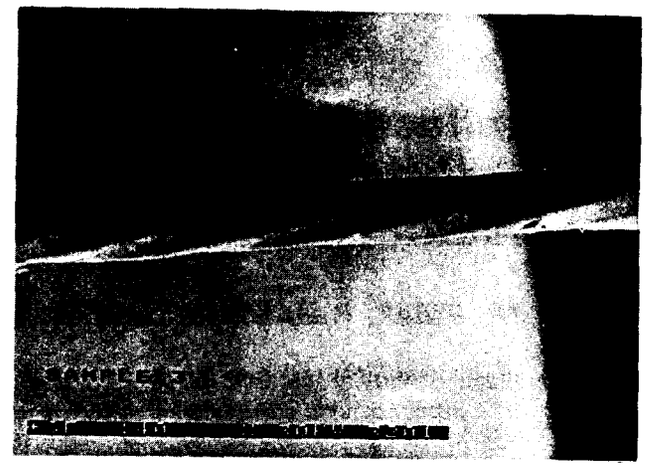

Figure 3 Microphotograph of sample 3

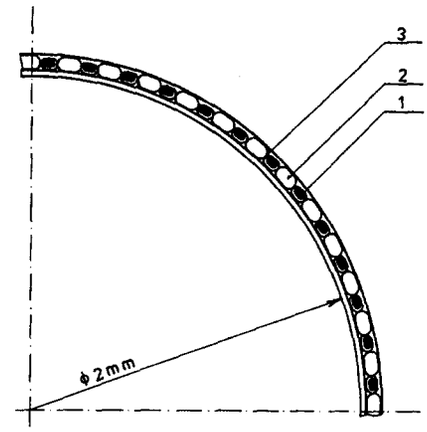

Figure 4 Cross-section of samples 4 and 5: 1, CFTH-14 monofilament; 2, copper wire (sample 4) or constantan wire (sample 5); 3, Pb–Sn solder

Experimental results

Current–voltage characteristic measurements were made in liquid helium at 4.2 K using the standard four-probe method in a perpendicular magnetic field. The electric field was calculated as $E = U/\Delta L$, where ΔL is the distance between the potential taps along the sample axis.

The *E–I* characteristics of sample 1 are shown in *Figure 5*. To compare these characteristics with those obtained on one separate copper-stabilized straight filament CFTH-14, in *Figure 5* the current corresponding to one filament in sample 1 is plotted on the *x*-axis. In the case of the twisted model sample, the *E–I* characteristics deviate from the exponential form at lower electric fields than in the case of one straight filament. It was found that this deviation cannot be caused by the increased amount of normal metal (Pb–Sn solder) added to the filaments during sample fabrication.

In *Figure 6* current–voltage characteristics of samples 2 and 3 are presented. If measuring at increased current slightly higher characteristics were observed for $10^1\ \mu$V cm$^{-1} < E < 10^3\ \mu$V cm^{-1}. This hysteresis, shown in *Figure 6* for sample 2 at 4 T only, is due to the known heat transfer hysteresis. It should be noted that all *E–I* characteristics presented in this Paper were measured at decreasing current in the interval of the electric field where

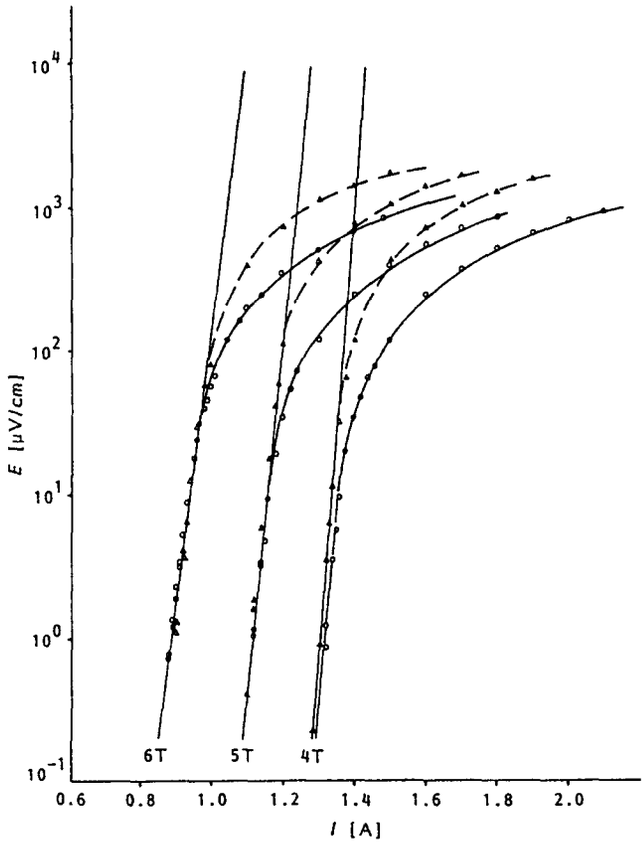

Figure 5 *E–I* characteristics at 6, 5 and 4 T of sample 1 compared with those of straight superconductor CFTH-14: ○, sample 1 (10 spirals with current multiplied by 0.1); △, one straight sample

hysteresis occurs. The influence of twisting on the *E–I* characteristics is the same as in the case of sample 1, i.e. *E–I* characteristics of the twisted sample deviate from the exponential at lower electric fields than in the case of the untwisted sample. However, samples 2 and 3 have different exponential portions of the slope for the *E–I* characteristics. The filament deformation during twisting introduces inhomogeneities, which are assumed to be responsible for the smaller slope of the characteristics measured on the twisted sample 3.

The influence of matrix resistance on the shape of *E–I* characteristics for samples 4 and 5 is shown in *Figures 7* and *8*. In the case of sample 5 (*Figure 8*), which has higher matrix resistance, the *E–I* characteristics have an exponential form as observed for one filament. On the other hand the *E–I* characteristics of sample 4 (*Figure 7*) which has lower matrix resistance, deviate from the exponential form at an electric field $E \sim 1$ to 5 μV cm^{-1}, dependent on the external magnetic field.

In *Figure 9* a comparison of *E–I* characteristics between twisted and untwisted real three dimensional multifilamentary composite is presented. The conductor was 0.0976 mm in diameter and contains 37 filaments (diameter, 10 μm; copper to superconductor ratio, 1.75; twist pitch, 1 mm). As seen in *Figure 9*, in low electric field region both conductors have the same critical currents, but at higher electric fields the *E–I* characteristics of the twisted conductor deviate from the exponential form at lower values of E than in the case of the untwisted one. In the case of fine filament superconductors comparison of *E–I* characteristics between untwisted and twisted samples is difficult because the process of twisting influences the intrinsic *E–I* characteristics of the single filaments.

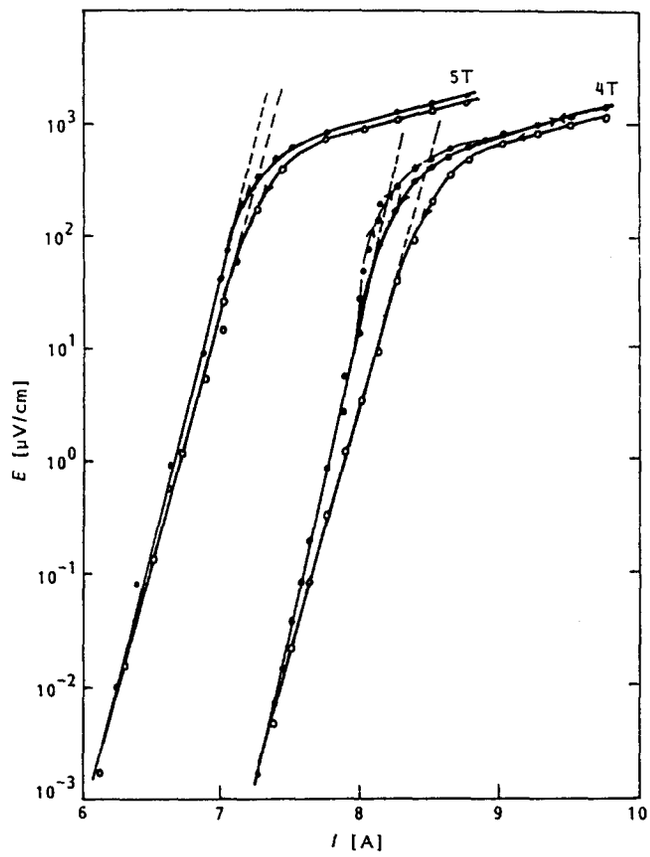

Figure 6 *E–I* characteristics of samples 2 and 3 at external magnetic fields 4 T and 5 T: ●, sample 2; ○, sample 3

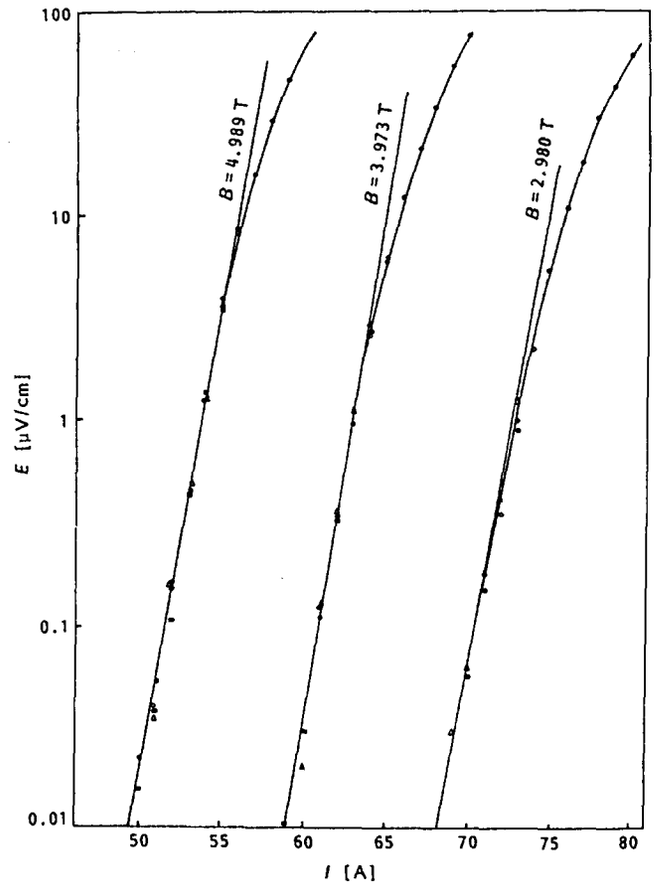

Figure 7 *E–I* characteristics of sample 4

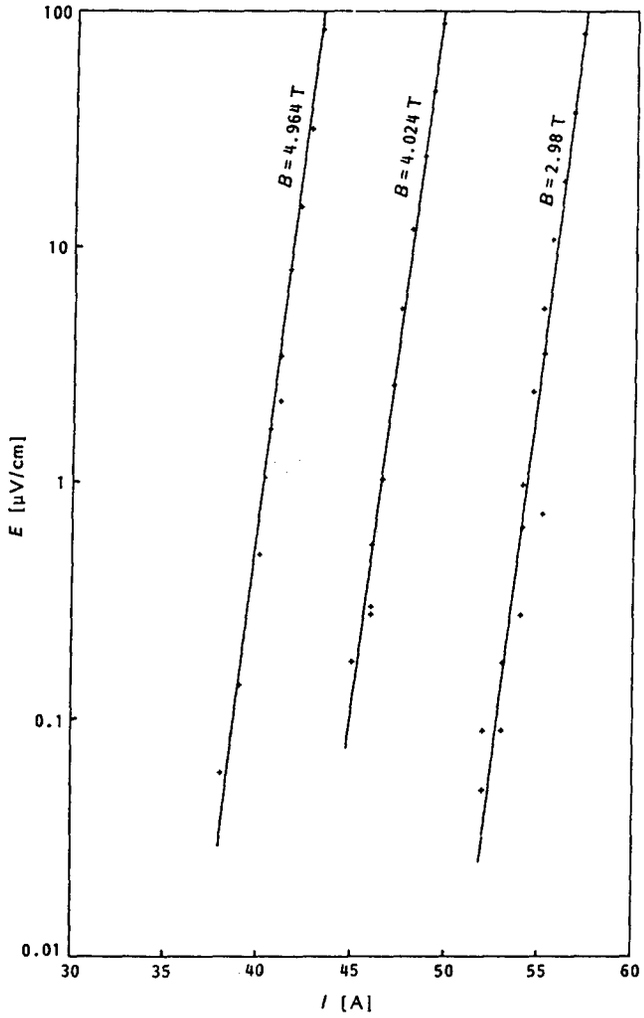

Figure 8 *E–I* characteristics of sample 5

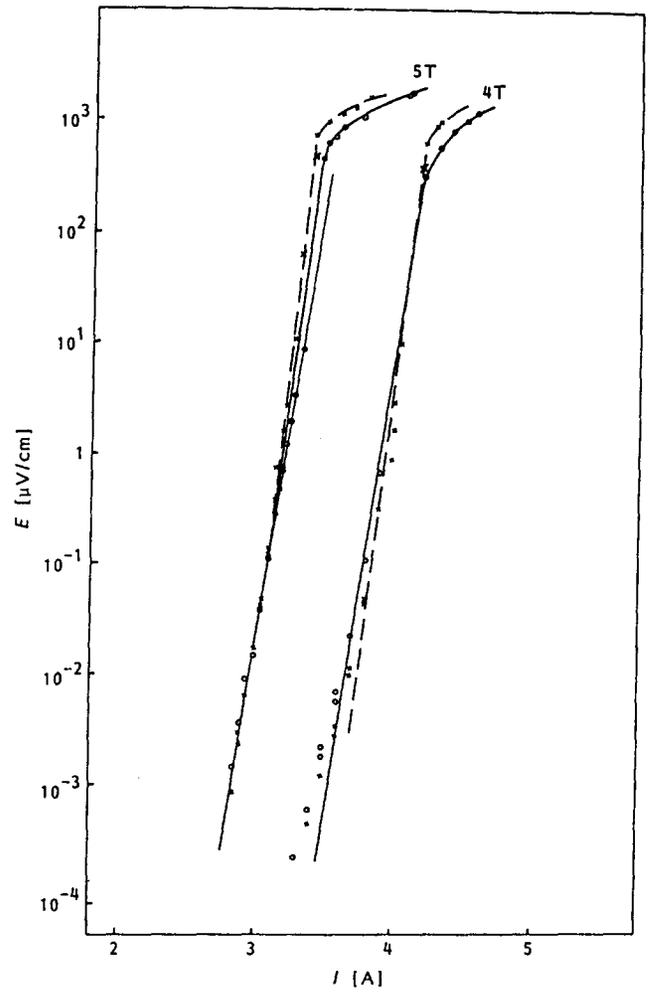

Figure 9 *E–I* characteristics of twisted and untwisted multifilamentary superconductor CFTH with 37 filaments: ×, untwisted; ○, twisted

Theoretical model

The observed *E–I* characteristics of twisted one layer model samples can be understood within the frame of the following simple macroscopic model. Let us consider a one layer multifilamentary superconductor with layer thickness d, radius R and twist pitch l_p (*Figure 10*). The conductor is placed in the coordinate system shown in *Figure 11a*, in an external magnetic field B perpendicular to the conductor axis. The composite is considered as a homogeneous anisotropic medium. The physical characteristics of such a medium are determined by averaging the characteristics of superconductor and normal metal across the areas containing a large number of superconducting filaments (*Figure 11*). Then for the current densities in direction along ($j_\parallel$) and perpendicular ($j_\perp$) to the superconducting filaments one can write

$$\vec{j}_\parallel = x_s \cdot j_s \frac{\vec{E}_s}{E_s} + x_n \sigma_n^\parallel \vec{E}_s \tag{1}$$

$$\vec{j}_\perp = \frac{1}{x_n} \sigma_n^\perp \vec{E}_n \tag{2}$$

where $\vec{E}_s$ and $\vec{E}_n$ are the electric field components along and perpendicular to the filaments. $\sigma_n^\parallel$, $\sigma_n^\perp$ are the normal metal matrix conductivities along and perpendicular to the filaments, respectively (see *Figure 11b*), and x_s, x_n are

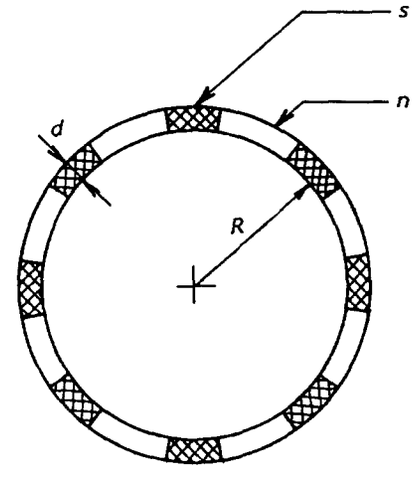

Figure 10 Cross-section of the model one-layer sample: s, superconductor; n, normal metal

the relative concentrations of the superconductor and normal metal ($x_n + x_s = 1$), respectively. For current–voltage characteristics the exponential expression[6] can be used

$$j_s = j_c + j_1 \ln \frac{E_s}{E_0} \tag{3}$$

where $j_c = j_c(B, T, \beta, E_0)$ is the critical current density

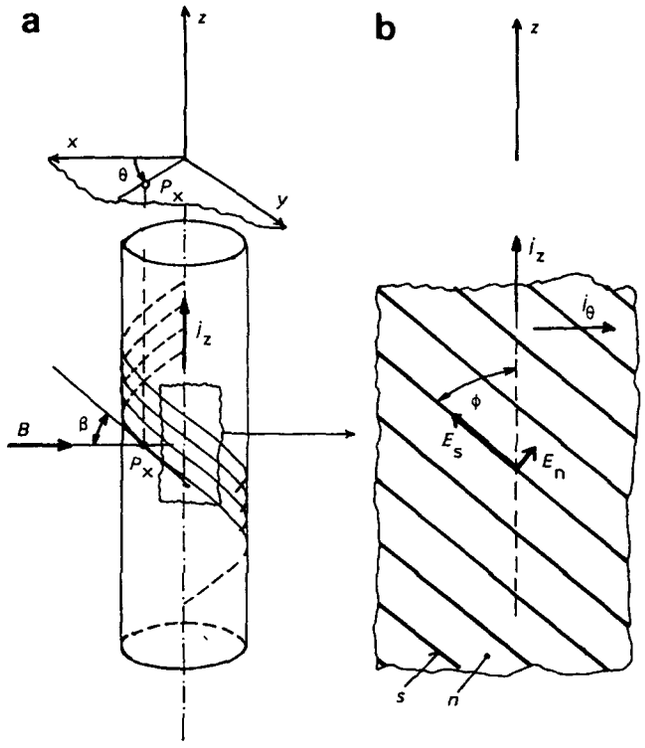

Figure 11 Orientation of the spiral sample in the coordinate system. s, superconducting filaments; n, normal metal matrix between the filaments and wire axis; E_s, E_n, electric fields along and perpendicular to the superconducting filaments, respectively.

corresponding to the electric field, E_0, the magnetic induction, B, the temperature, T, and the angle β between the magnetic field and wire axis. The parameter $j_1 = j_1(B, T, \beta)$ characterizes the slope of the E–I characteristics. Usually the value E_0 is from the interval 0.1–1 μV cm^{-1}. The angle φ is defined by the equation

$$\beta = \frac{\pi}{2} - \varphi \tag{4}$$

and the dependence $j_c(\varphi)$ is taken in the form

$$j_c(\varphi) = j_c(0)[1 + f(\varphi)]$$

From the symmetry of the problem it follows that $f(\varphi) = f(-\varphi)$. Note that for the filaments used in the experiment (CFTH-14) in the interval $0 < \varphi < \pi/3$ the function $f(\varphi)$ has the form[6] $f(\varphi) = 0.75\ \varphi^2(1 + \varphi^2)$. Because of the filament spirality the angle φ is determined by the angle θ (*Figure 11a*). The dependence $\varphi(\theta)$ is given by the equation

$$\sin \varphi = \sin \Phi \cdot \sin \theta \tag{5}$$

where Φ is the angle characterizing the filament spirality (see *Figure 11b*)

$$\tan \Phi = \frac{2\pi R}{l_p} \tag{6}$$

From the symmetry of the problem one has $\vec{E} = \vec{E}(\theta)$, $\vec{j} = \vec{j}(\theta)$. In this case using Maxwell equation rot $\vec{E} = 0$ and continuity equation div $\vec{j} = 0$ one can obtain that

$$E_z = E = \text{const} = \frac{U}{l} \tag{7}$$

$$j_\theta = \text{const} \tag{8}$$

where U is the voltage, l is the sample length, j_θ is asimuthal current density component with respect to conductor axis (see *Figure 11*).

E can be written as

$$E = \frac{U}{l} = \frac{1}{l_p}\int_0^{l_p} \hat{E}_s \mathrm{d}\vec{l} = \frac{R}{l_p \sin \Phi}\int_0^{2\pi} E_s \mathrm{d}\theta = \frac{1}{\cos \Phi}\bar{E}_s \tag{9}$$

where

$$\bar{E}_s = \frac{1}{2\pi}\int_0^{2\pi} E_s(\theta)\ \mathrm{d}\theta$$

and

$$\int \hat{E}_s \mathrm{d}\vec{l}$$

is the integral along the superconducting filament. In the following all the average values of an arbitrary function $g = g(\theta)$ shall be taken as

$$\bar{g} = \frac{1}{2\pi}\int_0^{2\pi} g(\theta)\mathrm{d}\theta.$$

From Equation (9) one has

$$\hat{E}_s = E \cos \Phi \tag{10}$$

Because

$$E = E_z = E_s \cos \Phi - E_n \sin \Phi \tag{11}$$

one has

$$\hat{E}_n = -E \sin \Phi \tag{12}$$

Let us determine now the average value of the current density j as

$$j = \frac{I}{A_n + A_s} \tag{13}$$

where I is the current flowing in the composite, and A_s and A_n are the cross-sections of all the superconducting and normal metal elements respectively. Then

$$\bar{j}_z = \frac{I \cos \Phi}{A_n + A_s} = j \cos \Phi \tag{14}$$

Because

$$j_z = j_\parallel \cos \Phi - j_\perp \sin \Phi \tag{15}$$

one can obtain

$$\bar{j}_z = j \cos \Phi = \bar{j}_\parallel \cos \Phi - \bar{j}_\perp \sin \Phi \tag{16}$$

From Equation (16) and using Equations (12) and (2)

$$\bar{j}_\parallel = j + \bar{j}_\perp \tan \Phi = j - \frac{\sigma_n^\perp E}{x_n} \sin \Phi \tan \Phi \tag{17}$$

In order to find the $E_s(\theta)$ dependence Equation (8) can be used, from which it follows that

$$j_\theta = \text{const} = j_\parallel \sin \Phi + j_\perp \cos \Phi = \bar{j}_\parallel \sin \Phi + \bar{j}_\perp \cos \Phi$$

or

$$j_\parallel = \bar{j}_\parallel + (\bar{j}_\perp - j_\perp)\cot\Phi = j - \frac{\sigma_n^\perp E}{x_n \cos \Phi} - \frac{\sigma_n^\perp E_n}{x_n \tan \Phi} \tag{18}$$

From Equation (11)

$$E_n = \frac{1}{\tan \Phi} E_s - \frac{1}{\sin \Phi} \frac{j_\parallel = \bar{j}_\parallel + (\bar{j}_T - j_T}{\mathrm{c}} \tag{19}$$

Inserting Equation (19) into Equation (18) the following can be obtained

$$j_{\parallel} = j - \frac{\sigma_n^{\perp} E_s}{x_n \tan^2 \Phi} + \frac{\sigma_n^{\perp} E}{x_n} \frac{1 - \tan^2 \Phi}{\cos \Phi \tan^2 \Phi} \tag{20}$$

Using Equations (20), (1) and (3) one obtains the following transcendental equation

$$j + \frac{\sigma_n^{\perp} E}{x_n} \frac{1 - \tan^2 \Phi}{\cos \Phi \tan^2 \Phi} - x_s j_c(\theta) = x_s j_1 \ln \frac{E_s}{E_0} + x_n \sigma_n^{\parallel} E_s + \frac{\sigma_n^{\perp} E_s}{x_n \tan^2 \Phi} \tag{21}$$

from which it is possible to determine the $E_s(\theta)$ dependence. For the solution of Equation (21) $E_s(\theta)$ was in the form

$$E_s = E_0 \cdot p \cdot e^{[-g]} \tag{22}$$

where

$$p = \exp \left\{ \frac{j - x_s j_c(\theta)}{x_s j_1} + \frac{\sigma_n^{\perp} E}{x_n x_s j_1} \frac{1 - \tan^2 \Phi}{\cos \Phi \tan^2 \Phi} \right\} \tag{23}$$

and $g(\theta)$ is the function to be determined.
Inserting Equations (22) and (23) into Equation (21) the following equation for $g(\theta)$ is found

$$g \exp[g] = p \frac{\sigma_n^{\perp} E_0}{x_n x_s j_1 \tan^2 \Phi} \left\{ 1 + \frac{\sigma_n^{\parallel}}{\sigma_n^{\perp}} x_n^2 \tan^2 \Phi \right\} \tag{24}$$

Introducing the following designation

$$\gamma_{\perp} = \frac{\sigma_n^{\perp} E_0}{j_1} \frac{1}{x_s x_n \tan^2 \Phi} \tag{25}$$

$$\gamma_{\parallel} = \frac{\sigma_n^{\parallel} E_0}{j_1} \frac{x_n}{x_s} \tag{26}$$

Note, that in real composites

$$\frac{\gamma_{\parallel}}{\gamma_{\perp}} = \frac{\sigma_n^{\parallel}}{\sigma_n^{\perp}} x_n^2 \tan^2 \Phi \ll 1$$

and $\gamma_{\parallel}, \gamma_{\perp} \ll 1$. Using Equations (25) and (26), Equation (24) takes the form

$$g \exp[g] = p(\gamma_{\parallel} + \gamma_{\perp}) \tag{27}$$

Now the condition $\bar{E}_s = E \cos \Phi$ and Equation (22) can be used to give

$$\overline{p \exp[-g]} = \cos \Phi \frac{E}{E_0}$$

or

$$\bar{g} = (\gamma_{\parallel} + \gamma_{\perp}) \cos \Phi \frac{E}{E_0} \tag{28}$$

From Equation (28) one has

$$\frac{E}{E_0} = \frac{\bar{g}}{\cos \Phi (\gamma_{\parallel} + \gamma_{\perp})} \tag{29}$$

Writing $j_c(\theta)$ in the form

$$j_c = j_c(0)\{1 + f[\varphi(\theta)]\}$$

it seems suitable to present the equation for determination of the function $g(\theta)$ in the following way

$$g \exp[g] = \exp\{a - A.f[\varphi(\theta)]\} \tag{30}$$

where

$$a = i + \frac{E}{E_0} \gamma_{\perp} \frac{1 - \tan^2 \Phi}{\cos \Phi} + \ln \frac{\gamma_{\parallel} + \gamma_{\perp}}{\alpha} \tag{31}$$

$$i = \frac{j - \tilde{j}_c(0)\, x_s}{j_1 x_s} \tag{32}$$

$$\tilde{j}_c(0) = j_c(0) + j_1 \ln \frac{1}{\alpha} \tag{33}$$

$$\alpha = \frac{2}{\sin \Phi \cos \Phi} \sqrt{\frac{1}{3\pi A}} \tag{34}$$

$$A = \frac{j_c(0)}{j_1} \gg 1 \tag{35}$$

$j_c(0)$ is the critical current density of a single spiral filament in a magnetic field perpendicular to the spiral axis[6].

Then the E–I characteristics of the one layer composite can be determined in the following way. For a given value of a and using Equation (30) the functions $g(\theta, a)$ and $g(a)$ can be determined. Then from Equation (29) the electric field E can be determined. If the value of E using Equation (31) is known the corresponding value of i can be found. The calculated dependences of log E/E_0 on i are shown in *Figure 12*. It is seen that increasing the value of $\gamma_{\perp}$, (i.e. the normal metal conductivity $\sigma_n^{\perp}$) causes the E–I characteristic deviation from the exponential form at lower values of E. This is in good agreement with our experiments on samples 4 and 5 (see *Figures 7* and *8*).

Note that the E–I characteristic for one spiral filament is give by Equation (29) if $\sigma_n^{\perp} = 0$ and $\gamma_{\perp} = 0$.

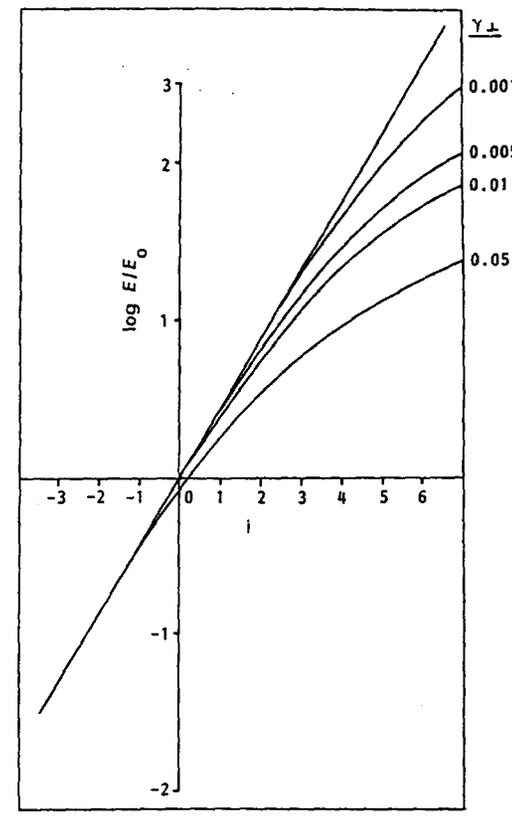

Figure 12 Dependence of log E/E_0 on i for different values of $\gamma_{\perp}$ (theoretical calculations)

In this case

$$\frac{E}{E_0} = \frac{\bar{g}}{\cos \Phi \, \gamma_{\parallel}} \tag{36}$$

and

$$i = a - \ln \frac{\gamma_{\parallel}}{\alpha} \tag{37}$$

Writing the expressions for E_s/E and E_n/E, using Equations (11), (22), (27) and (29) one obtains

$$\frac{E_s}{E} = \cos \Phi \frac{g}{\bar{g}} \tag{38}$$

$$\frac{E_n}{E} = \frac{1}{\sin \Phi} \left\{ \cos^2 \Phi \frac{g}{\bar{g}} - 1 \right\} \tag{39}$$

The dependences of E_s/E and E_n/E on θ are given in *Figure 13*. Note, that from Equations (2), (15), (18) and (39) it follows, that

$$j_z = j \cos \Phi + \frac{\sigma_n^{\perp} E}{x_n \tan^2 \Phi} \left(1 - \frac{g}{\bar{g}} \right) \tag{40}$$

It means that the amplitude of j_z distribution is

$$\delta j_z = \frac{\sigma_n^{\perp} E}{x_n \tan^2 \Phi} \frac{g_{max}}{\bar{g}}$$

From Equation (30) it is seen that $g(\theta)$ function acquires non-zero values in the intervals $|\theta - \pi| \leqslant \alpha \ll 1$
Then

$$\frac{g_{max}}{\bar{g}} \approx \frac{1}{\alpha} \gg 1 \text{ and}$$

$$\frac{\delta j_z}{x_s j_1} \approx \frac{\gamma_{\perp}}{\alpha} \tag{41}$$

Because $\alpha \ll 1$ the relation $\gamma_{\perp}/\alpha$ can be either higher or lower than 1, depending on the relation between $\gamma_{\perp}$ and α.

In the analysis of the limiting case, when at all angles θ the function $g(\theta) \ll 1$, or as seen from Equation (31), $a < 0$, then from Equation (30) it follows

$$g \approx \exp\{a - A f[\varphi(\theta)]\} \tag{42}$$

and

$$\bar{g} \approx \alpha \cos \Phi \exp \{a\} \tag{43}$$

Substituting Equation (43) into Equation (28) and using Equation (37) one can find the current–voltage characteristics of the one layer twisted composite in the form

$$i = \ln \frac{E}{E_0} \tag{44}$$

The condition of application (44) is the inequality

$$\frac{E}{E_0} \ll \frac{\alpha}{\gamma_{\parallel} + \gamma_{\perp}} \tag{45}$$

In such a way, as long as the condition in Equation (45) is fulfilled, E–I characteristics of the composite do not differ from those of the individual filament.

Conclusions

By twisting a multifilamentary NbTi composite superconductor periodic inhomogeneities of critical current density are introduced into the filaments. The inhomogeneities are due to the change of the angle between filament axis and the external magnetic field; thus they originate from the filament geometry.

On the basis of experimental analysis of the electric field and critical current density along a separated spiral filament several model conductors have been prepared, on which the influence of these inhomogeneities on E–I characteristics have been demonstrated. A theoretical model for explaining the form of E–I characteristics in the case of a one layer model conductor has been developed.

It has been shown that this theoretical model qualitatively explains the observed E–I characteristics quite well. It can be concluded that the current transfer through the

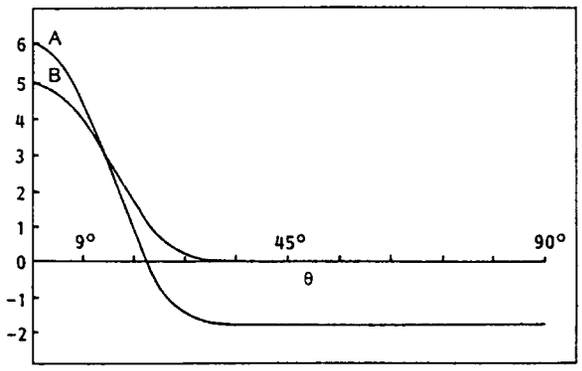

Figure 13 Dependence of theoretical values of E_n/E (*A*) and E_s/E (*B*) on θ

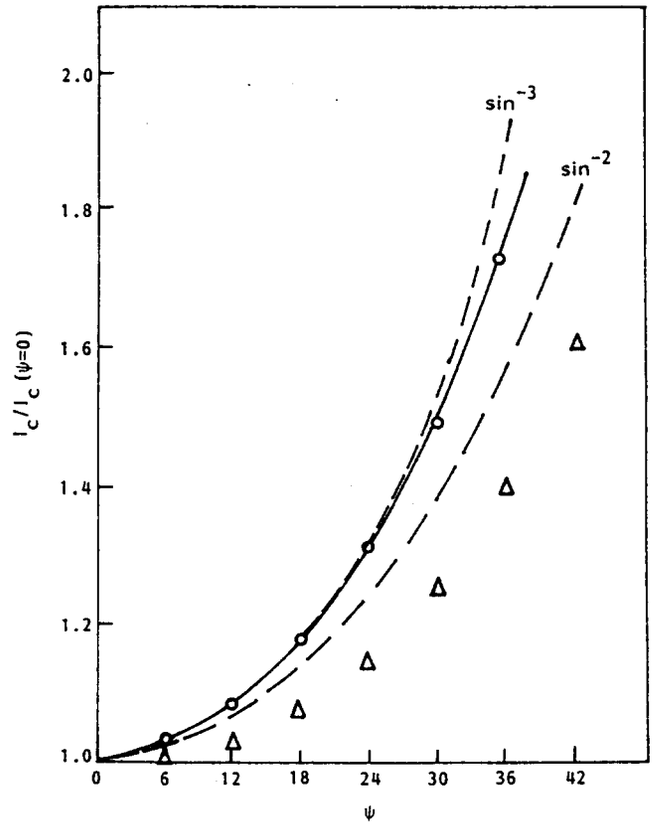

Figure 14 Angular dependence of critical current density: △, NbTi filament 36 μm in diameter; ○, NbTi filament 4 μm in diameter

normal metal matrix in twisted multifilamentary composite causes deviation of the *E–I* characteristics of the composite from that of the individual filaments. This effect arises even in the case of twisted filaments, which have a constant cross section and are free of metallurgical inhomogeneities. One can suppose that also in the case of real, i.e. three-dimensional, composites, with several filament layers, such an effect arises, but in this case current transfer also occurs in a radial direction. The theoretical analysis of such a real three-dimensional composite is substantially more complicated.

From the given analysis it follows, that the critical current density inhomogeneities introduced by the spiral form of filaments are also a function of angular dependence of the critical current density.

In the present work results are obtained for model conductors made of relatively thick filaments. Angular dependence of the wire used in these experiments compared with those obtained on 4 μm NbTi filament is shown in *Figure 14*. It is seen, that the decrease of the filament diameter causes substantial increase of the angular dependence of j_c. As a consequence one can expect, that the effects observed here can be much more pronounced in composites with finer filaments.

Acknowledgements

The authors are very grateful to L. Vencel for preparing the samples and to J. Talapa for the experimental assistance.

References

1 **Ekin, J.W.** *Cryogenics* (1987) **27**, 603
2 **Hampshire, D.P. and Jones, H.J.** *Phys C* (1987) **20**, 3533
3 **Hampshire, D.P. and Jones, H.J.** *Cryogenics* (1987) **27**, 608
4 **Warnes, W.H. and Larbalestier, D.C.** *Appl Phys Lett* (1986) **48**, 1403
5 **Warnes, W.H.** *J Appl Phys* (1988) **63**, 1651
6 **Polák, M., Mints, R.G., Majoroš, M. and Hlásnik, I.** *Cryogenics* (1987) **27**, 183